EasyChair Preprint

№ 6271

# A New Non-Stationary 3D Channel Model with Time-Variant Path Gains for Indoor Human Activity Recognition

Rym Hicheri, Ahmed Abdelgawwad and Matthias Pätzold



August 10, 2021

# A New Non-Stationary 3D Channel Model with Time-Variant Path Gains for Indoor Human Activity Recognition

R. Hicheri, A. Abdelgawwad, and M. Pätzold

Faculty of Engineering and Science, University of Agder, NO-4898 Grimstad, Norway

**ARTICLE HISTORY**
Compiled November 5, 2020

**ABSTRACT**
This paper introduces a new three-dimensional channel model to describe the propagation phenomenon taking place in indoor environments, equipped with a multiple-input multiple-output system, in the presence of a single moving person. Specifically, assuming that the person is modelled by a cluster of moving point scatterers, which act as relays, we derive the time-variant transfer function with time-variant path gains, time-variant Doppler shifts, and time-variant path delays. Then, we analyse the effect of the motion of the person on the spectrogram and the time-variant mean Doppler shift. Simulation results are presented to illustrate the proposed channel model.

**KEYWORDS**
Indoor propagation, non-stationary channels, cluster of moving scatterers, human activity recognition.

## 1. Introduction

With the expectation that the elderly population will triple in the next 30 years [United Nations (Oct. 2015)], there has been great interest in the study of home care systems based on human activity recognition, tracking, and classification techniques. A review of the literature shows that human activity recognition systems utilize two major techniques: wearable inertial measurement units and video surveillance [Jobanputra, Bavishi, and Doshi (2019)]. The main drawbacks of these systems are: the person may forget to wear the sensors-based devices and/or go outside the cameras' coverage area [Seneviratne et al. (4th Quart., 2017)]. Non-wearable radio-frequency (RF)-based systems have been introduced to overcome the drawbacks of the aforementioned systems [Liu, Liu, Chen, Wang, and Wang (Aug. 2019)]. These RF-based devices track and monitor indoor human activities by exploiting the effects of the human motion on the Doppler characteristics of the transmitted RF signals.

A three-dimensional (3D) non-stationary channel model with constant path gains has been reported in [Abdelgawwad and Pätzold (Apr. 2019)], where the body segments of the moving person have been modelled by a cluster of synchronized moving scatterers. The authors analysed the effects of the motion of the person on the spectrogram of the complex channel gain. A 3D non-stationary channel model with a stochastic trajectory model has been presented in [Borhani and Pätzold (Nov. 2018)]

CONTACT R. Hicheri Email: rym.hicheri@uia.no

which incorporates time-variant (TV) path gains that change with the distance of the moving person from the transmitter/receiver. In [Borhani and Pätzold (Nov. 2018)], the TV path gains are determined according to the path loss model in [Phillips, Sicker, and Grunwald (1st Quart., 2013)] by considering the sum of the travelled distances between the scatterers and the transmitter/receiver. This assumption does not match the results of several studies, in which the effects of electromagnetic fields on the human body have been investigated [Council et al. (1993a, 1993b); Federal Public Service (Jan. 2019); Mahmoudinasab, Sanie-Jahromi, and Saadat (Jun. 2016)]. According to the aforementioned references, in the presence of low-frequency electromagnetic fields, an electric current is generated in the human body which is generally referred to as "induced current". As a result, the different body segments of the moving person are assumed to play the role of relays, which redirect the transmitted RF signal. In this case, the mean power of the TV path gain of each multipath component is modelled according to the free-space path loss model [Phillips et al. (1st Quart., 2013)], which depends on the product of the distance between the transmit antenna and the scatterer (body segment) and the distance between the scatterer and the receive antenna.

The goal of this work to address this problem. To do so, we present a new generic non-stationary 3D indoor channel model, where the different body segments of the moving person are assumed to play the role of moving relays. In this case, we present an expression for the time-variant transfer function (TVTF) with TV path gains and TV path delays, where the mean power of TV path gains is modelled by the free-space path loss model [Phillips et al. (1st Quart., 2013)]. The analysis of the influence of the motion of different body segments on the Doppler characteristics of the channel is conducted by means the spectrogram of the TVTF and the TV mean Doppler shift. Simulation results are presented to illustrate the proposed channel model.

The remaining of this paper is organised as follows. Section II discusses the indoor propagation scenario with the cluster of moving scatterers. The derivation of the TVTF of the received RF signals is presented in Section III. Section IV presents some numerical results and Section V concludes the paper.

## 2. Scenario Description

As illustrated in Fig. 1, we consider a rectangular cuboid room. The room of length $A$, width $B$, and height $H$ is equipped with an $N_T \times N_R$ MIMO communication system, where $N_T$ denotes the number of transmit antennas $A_j^T$ $(j = 1, \ldots, N_T)$ and $N_R$ designates the number of receive antennas $A_i^R$ $(i = 1, \ldots, N_R)$. There are several stationary (fixed) objects (e.g., walls, furniture, and decoration items) and a single moving person. The moving person is modelled by a cluster of moving scatterers, where each single point scatterer (★) represents a segment of the human body such as head, shoulders, arms, etc.

The corresponding geometrical 3D channel model shown in Fig. 2 is the starting point for modelling the indoor propagation phenomenon. Each transmit (receive) antenna element $A_j^T$ $(A_i^R)$ is located at the coordinates $(x_j^T, y_j^T, z_j^T)$ $((x_i^R, y_i^R, z_i^R))$, $j = 1, 2, \ldots, N_T$ $(i = 1, 2, \ldots, N_R)$. Here, we assume the presence of LOS components. The fixed objects between $A_i^T$ and $A_j^R$ are modelled by $K_{ij}$ fixed point scatterers (•), denoted by $S_{k_{ij}}^F$, $k_{ij} = 1, 2, \ldots, K_{ij}$. On the other hand, every body segment of the moving person is modelled by a single point moving scatterer (★), denoted by $S_n^M$ $(n = 1, 2, \ldots, M)$, which is located at the TV position $(x_n(t), y_n(t), z_n(t))$. Single-

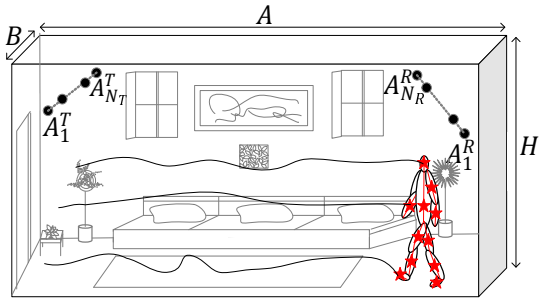


**Figure 1.** A single moving person (modelled by a cluster of moving scatterers) walks in a room equipped with a MIMO system and several fixed (stationary) objects.

bounce scattering is assumed when modelling the fixed and moving scatterers.

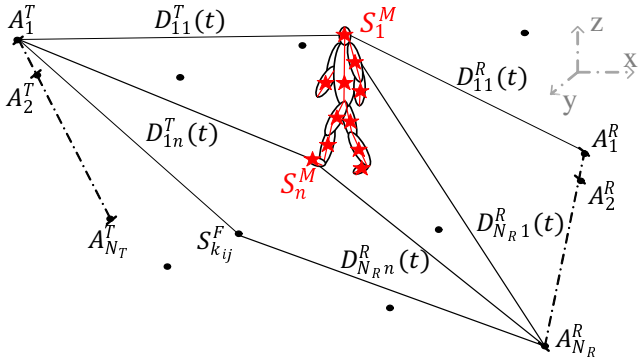


**Figure 2.** The 3D geometrical model for an $N_T \times N_R$ MIMO channel with fixed (•) and moving scatterers (★).

Together with considering TV path gains and TV path delays, the other novelty of this work is that the human body segments are assumed to play the role of relays, which redirect the transmitted radio wave. This is motivated by the fact that low-frequency electromagnetic fields have been shown to induce (in)perceivable electric currents in the human body, which in turn can cause a tingling sensation depending on the frequency range [Council et al. (1993a, 1993b); Federal Public Service (Jan. 2019); Mahmoudinasab et al. (Jun. 2016)]. In other words, when the transmitted RF signal impinges on a body segment (moving scatterer), then an electric current induced, which retransmits the RF signal in all directions. In the presence of these induced currents, the human body segments (moving scatterers) play the role of relays. In this case, the free-space path loss model [Phillips et al. (1st Quart., 2013)] states that the power $P^R_{in}(t)$ received at the $i$th receive antenna $A^R_i$ after being relayed by the $n$th moving scatterer $S^M_n$ is given by

$$P^R_{in}(t) = a_n^2 C^2 \left[D^R_{in}(t) \times D^T_{jn}(t)\right]^{-\gamma} \tag{1}$$

where the quantity $C$ depends on the transmit/receive antenna gain, the transmission power, and the wavelength [Phillips et al. (1st Quart., 2013)] and $\gamma$ is the path loss exponent which is equal to 2 in free space and between 1.6 a1.8 in indoor environments. The parameter $a_n$ describes the weight (contribution) of the $n$th moving scatterer $S^M_n$ with respect to the total propagation phenomenon, with $\sum_{n=1}^{M} a_n^2 = 1$. Here, the quantity $D^T_{jn}(t)$ ($D^R_{in}(t)$) represents the TV distance between the $j$th ($i$th) transmit

(receive) antenna $A_j^T$ ($A_i^R$) and the $n$th moving scatterer $S_n^M$. According to Fig. 2, the TV distances $D_{jn}^T(t)$ and $D_{in}^R(t)$ can be expressed as

$$D_{jn}^T(t) = \left[\left(x_n(t)-x_j^T\right)^2+\left(y_n(t)-y_j^T\right)^2+\left(z_n(t)-z_j^T\right)^2\right]^{1/2} \quad (2)$$

and

$$D_{in}^R(t) = \left[\left(x_i^R-x_n(t)\right)^2+\left(y_i^R-y_n(t)\right)^2+\left(z_i^R-z_n(t)\right)^2\right]^{1/2} \quad (3)$$

respectively.

## 3. The 3D Non-Stationary Channel Model

According to Fig. 2, the TVTF $H_{ij}(f',t)$ of the sub-channel between $A_j^T$ and $A_i^R$ can be expressed as

$$H_{ij}(f',t) = \sum_{n=1}^{M} c_{ijn}(t)\exp\left(j\left(\theta_{ijn}-2\pi f'\tau'_{ijn}(t)\right)\right)+\sum_{k=0}^{K_{ij}} c_{k_{ij}}\exp\left(j\left(\theta_{k_{ij}}-2\pi f'\tau'_{k_{ij}}\right)\right). \quad (4)$$

The first part of (4) describes the effects of the motion of the cluster of scatterers (representing the moving person). Here, the quantities $c_{ijn}(t)$ and $\tau'_{ijn}(t)$ are the TV path gain and TV path delay of the $n$th moving scatterer $S_n^M$ ($n = 1, 2, \ldots, M$), respectively. These parameters are given by

$$c_{ij}(t) = \sqrt{P_{in}^R(t)} = a_n C\left[D_{in}^R(t)\times D_{jn}^T(t)\right]^{-\gamma/2} \quad (5)$$

and

$$\tau'_{ijn}(t) = \frac{D_{jn}^T(t)+D_{in}^R(t)}{c_0}. \quad (6)$$

The quantity $c_0$ denotes the speed of light. The initial phases of the channel, denoted by $\theta_{ijn}$ are modelled by independent and uniformly distributed (i.i.d.) random variables which are uniformly distributed over the interval $[0, 2\pi)$.

The second sum of (4) models the multipath propagation effect resulting from the fixed scatterers. Each fixed scatterer $S_{k_{ij}}$ is described by a constant path gain $c_{k_{ij}}$, a constant path delay $\tau'_{k_{ij}}$, and a constant phase $\theta_{k_{ij}}$, $k = 1, \ldots, K_{ij}$. The LOS component, which doesn't experience any Doppler effect, can be modelled by a fixed scatterer $S_0^F$ ($k = 0$), with a constant path gain $c_{0_{ij}}$ and a constant delay $\tau_{0_{ij}}$. The phases $\theta_{k_{ij}}$ are modelled by i.i.d. random variables with a uniform distribution over the interval $[0, 2\pi)$. For simplicity, the overall effect of the fixed scatterers, i.e., the second sum of (4), is replaced by a single complex term $c_{ijF}(f')\exp[j(\vartheta_{ijF}(f'))]$, with an envelope $c_{ijF}(f')$ and a phase $\vartheta_{ijF}(f')$. These quantities are expressed as $c_{ijF}(f') = \{[\sum_{k=0}^{K_{ij}} c_{k_{ij}}\cos(\theta_{k_{ij}}-2\pi f'\tau'_{k_{ij}})]^2+[\sum_{k=0}^{K_{ij}} c_{k_{ij}}\sin(\theta_{k_{ij}}-2\pi f'\tau'_{k_{ij}})]^2\}^{1/2}$ and $\vartheta_{ijF}(f') = \text{atan2}(\sum_{k=0}^{K_{ij}} c_{k_{ij}}\sin(\theta_{k_{ij}}-2\pi f'\tau'_{k_{ij}}), \sum_{k=0}^{K_{ij}} c_{k_{ij}}\cos(\theta_{k_{ij}}-2\pi f'\tau'_{k_{ij}}))$, respectively, where atan2)$\cdot$) is the inverse tangent function.

To visualize the influence of the moving person (cluster of scatterers), we consider the spectrogram $S_{ij}(f,t)$ of the TVTF $H_{ij}(f',t)$ using a Gaussian window [Abdelgawwad and Pätzold (Apr. 2019); Borhani and Pätzold (Nov. 2018)]. For short time intervals during which the coordinates $x_n(t)$, $y_n(t)$, and $z_n(t)$ of the moving scatterers $S_n^M$ $(n = 1, 2, \ldots, M)$ can be assumed to be constant, an approximate solution to the spectrogram $S_{ij}(f,t)$ of the TVTF $H_{ij}(f',t)$ can determined according to [(Borhani & Pätzold, Nov. 2018, Eqs. (17)−(20))]. From [Borhani and Pätzold (Nov. 2018)], the TV mean Doppler shift $B_{ij,H}^{(1)}(t)$ can be determined from the spectrogram $S_{ij}(f,t)$ using [(Borhani & Pätzold, Nov. 2018, Eq. (22))].

## 4. Simulation Results

In this section, we explore the propagation scenario described in Section 2 by studying the effect of the TV path gains on the spectrogram and the TV mean Doppler shift of the TVTF of the received RF signal. For brevity, the transmitter $T_X$ and the receiver $R_X$ are co-located on the ceiling of the room and equipped with a single antenna. A single walking person is considered in two different scenarios. In the first one, the person is represented by a single moving scatterer ($M = 1$) corresponding to the head. In the second one, the person is modelled by 6 moving point scatterers ($M = 6$) representing the major segments of the human body, namely, the head, the ankles, the wrists, and the waist. The trajectories of the different body segments are simulated according to [(Abdelgawwad & Pätzold, Apr. 2019, Section V)]. The person is initially located below to the $T_X$ and $R_X$ antennas and walks away from the antennas. The parameters $C$ and $\gamma$ are set to 1 and 1.6, respectively. The contribution of the fixed scatterers is removed by using a high-pass filter. For the remaining parameters as well as the scenario with constant path gains, we consider the same simulation parameters as in [(Abdelgawwad & Pätzold, Apr. 2019, Section V)].

Figs. 3(a) and (b) (Figs. 4(a) and (b)) depict the spectrogram $S_{11}(f,t)$ corresponding to Scenario I (Scenario II) while considering TV path gains and constant path gains, respectively. In Figs. 3 and 4, the Doppler frequencies caused by the walking activity have negative values because the propagation delays (total travelled distances) increase when the person is walking away from the $T_X$ and $R_X$ antennas. By comparing Figs. 3(a) and 4(a) (Figs. 3(b) and 4(b)), it can be observed that the resolution of the spectrogram is lower for Scenario II ($M = 6$). This is due to the presence of the spectrogram's cross-term (see [Abdelgawwad and Pätzold (Apr. 2019), Eq. (47)]). From Figs. 3(a) and 4(a), it can also be noted that the instantaneous power of the spectrogram decreases w.r.t. time $t$. This stems from the fact that when the person is moving away from the antennas, the TV distances $D_{1n}^T(t)$ and $D_{1n}^R(t)$ increase w.r.t. time $t$. In practice, this can be explained by the fact that by moving away from the $T_X$ and the $R_X$ antennas, the person is walking out of the range of the RF system. This is in contrast to what can be observed in Figs. 3(b) and 4(b), where the instantaneous power of the spectrogram remains constant, i.e., the range of the RF system is infinite.

To further investigate the effect of introducing TV path gains on the Doppler characteristics of channel, we present in Figs. 5(a) and (b) a comparison of the TV mean Doppler shifts $B_{11,H}^{(1)}(t)$ using TV path gains and constant path gains for Scenario I ($M = 1$) and Scenario II ($M = 6$), respectively. From Fig. 5(a), it is clear that for $M = 1$, the TV behavior of the path gains does not affect $B_{11,H}^{(1)}(t)$. This comes from

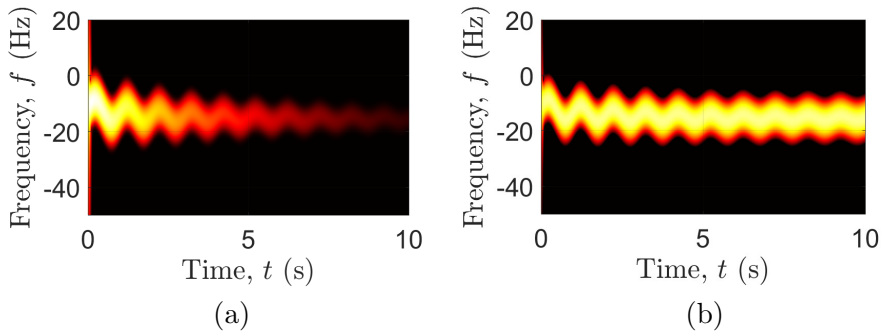


**Figure 3.** Spectrogram $S_{11}(f,t)$ for $M = 1$ with (a) TV path gains and (b) constant path gains.

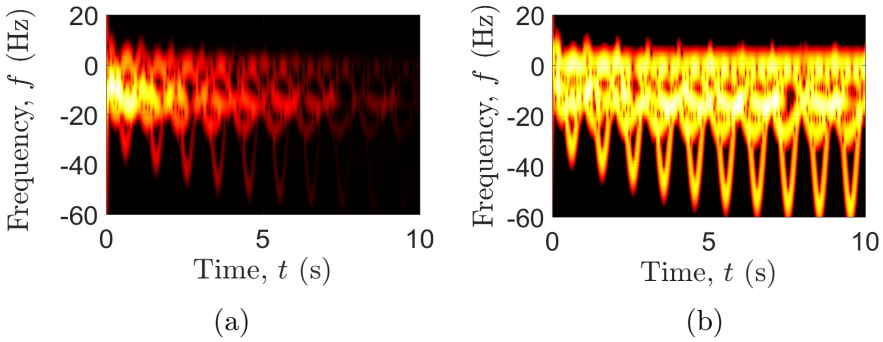


**Figure 4.** Spectrogram $S_{11}(f,t)$ for $M = 6$ with (a) TV path gains and (b) constant path gains.

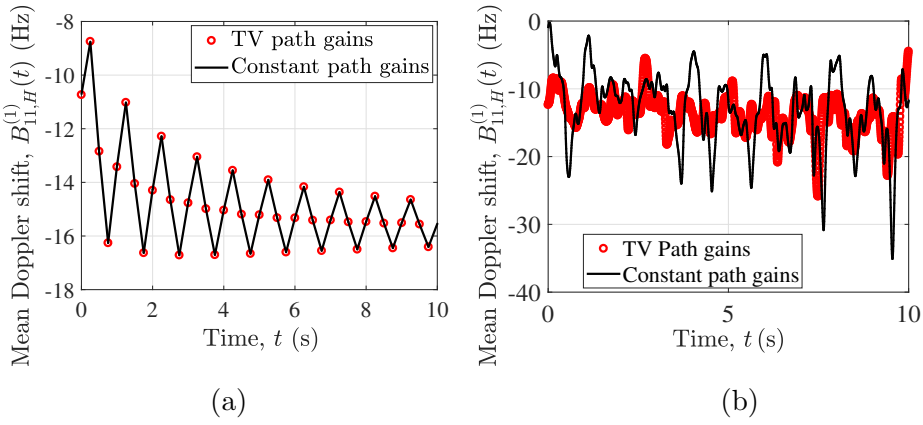


**Figure 5.** TV mean Doppler shift $B^{(1)}_{11,H}(t)$ for (a) $M = 1$ and (b) $M = 6$.

the fact that for $M = 1$, $B^{(1)}_{11,H}(t)$ reduces to the TV Doppler frequency $f_{11}(t)$ (see [Borhani and Pätzold (Nov. 2018), Eq. (21)]). The effect of the TV path gains can be clearly seen in Fig. 5(b) for $M = 6$. In fact, for $M > 1$, the TV path gains affect both the trend and the values of $B^{(1)}_{11,H}(t)$.

## Acknowledgement

This work was supported by the WiCare Project funded by the Research Council of Norway under grant number 261895/F20.

## References


Abdelgawwad, A., & Pätzold, M. (Apr. 2019). A 3D non-stationary cluster channel model for human activity recognition. In *IEEE 89th Veh. Technol. Conf. (VTC'19-Spring)* (pp. 1–7).

Borhani, A., & Pätzold, M. (Nov. 2018). A non-stationary channel model for the development of non-wearable radio fall detection systems. *IEEE Trans. Wireless Commun.*, *17*(11), 7718–7730.

Council, N. R., et al. (1993a). Effects of electromagnetic fields on organs and tissues. In *Assessment of the possible health effects of ground wave emergency network.* National Academies Press (US).

Council, N. R., et al. (1993b). Human laboratory and clinical evidence of effects of electromagnetic fields. In *Assessment of the possible health effects of ground wave emergency network.* National Academies Press (US).

Federal Public Service. (Jan. 2019). *Federal Public Service: Interaction between radiation and the human body.* (Accessed in: Mar. 2020. Available: https://www.health.belgium.be/en/interaction-between-radiation-and-human-body-article)

Jobanputra, C., Bavishi, J., & Doshi, N. (2019). Human activity recognition: A survey. *Procedia Computer Science*, *155*, 698–703.

Liu, J., Liu, H., Chen, Y., Wang, Y., & Wang, C. (Aug. 2019). Wireless sensing for human activity: A survey. *IEEE Commun. Surveys Tuts.*.

Mahmoudinasab, H., Sanie-Jahromi, F., & Saadat, M. (Jun. 2016). Effects of extremely low-frequency electromagnetic field on expression levels of some antioxidant genes in human MCF-7 cells. *Molecular Biology Research Commun.*, *5*(2), 77−85.

Phillips, C., Sicker, D., & Grunwald, D. (1st Quart., 2013). A survey of wireless path loss prediction and coverage mapping methods. *IEEE Commun. Surveys & Tuts.*, *15*(1), 255–270.

Seneviratne, S., et al. (4th Quart., 2017). A survey of wearable devices and challenges. *IEEE Commun. Surveys & Tuts.*, *19*(4), 2573–2620.

United Nations. (Oct. 2015). *United Nations: Transforming our world: the 2030 agenda for sustainable development.* (Accessed in: Mar. 2020. [Online]. Available: https://www.health.belgium.be/ en/interaction-between-radiation-and-human-body#article, report no.A/RES/70/1)